ISSN (Online):0493-2137

E-Publication: Online Open Access Vol: 56 Issue: 06:2023

DOI: 10.5281/zenodo.17275786

EFFECTS OF Ce/La nano-oxides IN SPENT TEA ACTIVATED CARBON (SAC-Ce/La) FOR THE REMOVAL OF DIBENZOTHIOPHENE (DBT) AND BENZOTHIOPHENE (BT) FROM A MODEL OIL

CHRISTOPHER NKANSAH*

University of North Dakota, Grand Forks ND, USA. *Corresponding Author Email: christopher.nkansah@und.edu

VICTOR OJO

University of North Dakota, Grand Forks ND, USA. Email: victor.ojo@und.edu

MAXWELL BAWUAH

University of North Dakota, Grand Forks ND, USA. Email: maxwell.bawuah@und.edu

ABIMBOLA OJO

Ladoke Akintola University of Technology, Nigeria. Email: abimbola-Ojo@outlook.com

ODUNOLA ODOFIN

University of North Dakota, Grand Forks ND, USA. Email: odunola.odofin@und.edu

Abstract

This study demonstrates the removal of benzothiophene (BT) and dibenzothiophene (DBT) from model oil by the impregnation of spent-tea activated-carbon (SAC) with nan-oxide of Ce/La to produce SAC-Ce/La. The sol-gel method was used to prepare the metal-oxide nanoparticles while the spent-tea was carbonized at 400 °C to give the SAC. Adsorbent characterization was determined. The removal efficiency of the SAC-Ce/La was high with a maximum adsorption capacity of 56.2 mg/g compared to the separate constituents (SAC and SAC-Ce). The improvement in the adsorbate uptake by the SAC-Ce/La can be ascribed to the presence of La ion in the adsorbent. The surface area and pore volume of the SAC-Ce/La that was used to adsorb the BT/DBT are 801.6 m²g⁻¹ and 1.12 cm³/g as obtained from BET analysis. Column and batch experiments conducted with the SAC-Ce/La showed a high breakthrough and absorptive capacity for BT/DBT. The results from equilibrium adsorption were best described by the Freundlich isotherm, while the adsorption kinetics of BT/DBT by SAC-Ce/La is best represented by the pseudo-second-order model. The thermal regeneration of SAC-Ce/La showed a sustainable adsorptive performance after 5-regeneration cycles. Therefore, the nano-oxides of Ce/La in the SAC-Ce/La can efficiently remove BT/DBT from a model fuel/oil.

Keywords: Activated Carbon; Dibenzothiophene; Benzothiophene; Model Oil; Nanoparticle.

Definition of Some Basic Terms

Parameter	Definition
q_e (mg/g)	Amount adsorbed at Ce (mg/L)
$q_m \text{ (mg/g)}$	Langmuir constant representing monolayer capacity:
K_F (mg/g) and n	Freundlich constants
C_o (mg/L)	initial concentration of the analytes
PŠO	Pseudo second order kinetic model
K_L (L/mg)	Langmuir constant.
R = 1	Indicates linearity,

ISSN (Online):0493-2137

E-Publication: Online Open Access Vol: 56 Issue: 06:2023 DOI: 10.5281/zenodo.17275786

k ₂ (g/mg minute)	pseudo-second-order adsorption rate constant
k_1 (Min ⁻¹)	Pseudo first-order kinetic model rate constant
C_e (mg/L)	Equilibrium concentration
SAC	Spent tea activated carbon
PFO	Pseudo first-order kinetic model
Ce/La	Nano-oxides of cerium and lanthanum

1. INTRODUCTION

When sulphur compounds undergo combustion, they usually produce SO_x emissions which may lead to serious health issues or in turn result in acid rain. The total sulphur content in crude oil lies between 0.04 and 6.0 wt. %, which also depends on the nature and source/origin of the fossil fuel [1, 2].

According to environmental standards/regulations, the concentrations of sulphur in diesel fuel should not be more than 10 ppm [3]. Petroleum refineries hydrodesulphurization technology (HDS) to reduce the sulphur content of hydrocarbon products in order to reduce the sulphur content of the fuel to an acceptable level [4]. However, due to the high temperature and pressure required, as well as the correspondingly high operating expenses, this technique is neither economical despite being somewhat effective in removing sulphur compounds. Various methods are being looked into in order to get over these operational challenges in order to obtain ultra-clean gasoline [5-6]. There are several desulphurization techniques which include biodesulphurization (BDS), Oxidative desulphurization (ODS) [3], hydrodesulphurization (HDS), extractive desulphurization (EDS) [7], precipitative desulphurization, extractive desulphurization, and adsorptive desulphurization (ADS) of fuels [8]. The HDS technique barely achieves high/complete removal of sulphur in diesel fuels which may in turn constitute negative impacts on the environment, economy, and health [9]. Furthermore, HDS is less efficient in removing compounds of sulphur such as dibenzothiophene (DBT). thiophene, and benzothiophene (BT) [10] and may require large amounts of expensive catalyst. Thus, it is important to produce an efficient, less expensive, viable adsorbent that can overcome these challenges.

Due to its ability to match moderate conditions (temperature and pressure) without requiring hydrogen, ODS is thought to be highly cost-effective [11]. The major drawback of ODS is a challenge with recycling sulfones, which are ODS by-products. Different organic solvents (extractants), including pyrrolidones, dimethylformamide and acetonitrile, are utilized in EDS, a selective sulphur removal process [12 -13]. Despite being used as extractants, organic solvents have a number of drawbacks which include low selectivity i.e., while being viable for the extraction of olefins and sulphur-containing compounds, they in turn reduce the quality of the fuel with an attendant increase in the fuel's volatility, toxicity, and flammability which violate the concept of green chemistry [7, 10].

On the other hand, adsorptive desulphurization (ADS), is one of the most researched alternative technologies which has the potential to replace or enhance traditional HDS.

ISSN (Online):0493-2137

E-Publication: Online Open Access Vol: 56 Issue: 06:2023

DOI: 10.5281/zenodo.17275786

Sulphur compounds are eliminated by adsorption in the ADS process using a specific adsorbent [14]. This indicates that the adsorbent is crucial to the process's selectivity, capacity, and sustainability (i.e., the tendency for adsorbent-regeneration). Chemical or physical adsorption can be used to remove sulphur, depending on how the adsorbent and the sulphur compounds interact [15]. The potential for ADS to be environmentally friendly, economical, and regenerative at ambient conditions, makes it an attractive approach. The biggest obstacles to ADS have been diffusion and selectivity restrictions [16]. The exploration of a wide spectrum of possible adsorbents with high sulphur capacity and selectivity has so received much interest in modern-day research. The textural characteristics of the adsorbents have a major impact on the efficacy of ADS. Pore volume, high surface area, stability, surface-active sites, number of mesopores and good structural strength are also beneficial features desired of the adsorbents [1, 8, 17].

Metal oxides are very reactive with sulphur compounds, especially thiols. The desulphurization potential of several metal oxides, including MnO₂, PbO₂, ArO₃, Al₂O₃, MgO₂, ZnO₂, and silica, in response to model oils have been reported. For the purpose of removing sulphur compounds from a model-oil, Song and Ma [18] presented a desulphurization process based on selective adsorption on transition metal-based adsorbents. Yang et al. [19] developed a metal-containing zeolite-based adsorbent for the removal of sulphur compounds removal from transportation fuel at ambient condition. Cu/ZnO/Al₂O₃ has also been investigated for its sulphur removal ability [20, 21]. Both studies highlighted the critical function of ZnO in stabilizing Cu/ZnO particles and preventing Cu metal agglomeration. For the purpose of removing thiophene from hydrocarbons, they improved the adsorptive characteristics of the Cu/ZnO/Al₂O₃ adsorbent. For the removal of sulphur compounds, a variety of adsorbents including mixed oxides [15], metal-exchanged zeolites [21], metal loaded alumina [19] etc. have been adopted in which strong sulphur chemisorption on zeolite Lewis's acid sites led to high sulphur removal capabilities in metal-exchanged zeolite-based adsorbents. In a study conducted by Shakirullah et al. [22], there was significant sulphur depletion by PbO₂ and MnO₂; the PbO₂ and MnO₂ brought about a maximum desulphurization of 60.28% and 58.55 %.

The oxides of La and Ce have shown high adsorptive performances for the removal of contaminants such as heavy metal, aromatics, dyes etc. due to their numerous pore size distribution, large surface area [14], catalytic activities, available polar sites [19], chemical resistance and reproducibility in terms of their degree of activation [23]. However, there are still some shortcomings such as their incomplete removal of sulphur compounds from model oils when used with metal oxides, hence the need to blend them with spent tea activated carbon (SAC).

SAC has shown a high surface area and adsorptive capacity, which can be regenerated easily [24]. Improving the properties of SAC with metal oxides, oxidizing agents, and metals, can also enhance its capacity, selectivity, and reactivity to compounds of sulphur [25]. Metal oxides such as Al₂O₃, MgO₂, La₂O₃, CeO₂ and ZnO₂ have been added to carbon materials to help improve their adsorptive properties [26]. The desulphurization

ISSN (Online):0493-2137

E-Publication: Online Open Access Vol: 56 Issue: 06:2023

DOI: 10.5281/zenodo.17275786

activity of SAC can be greatly increased by the metal oxides loaded on it [9]. The oxides of V, Co, Fe, Ni and Mn impregnated in AC displayed high SO₂ removal capacities particularly that impregnated with Fe and V [10].

Xiong et al. [26] loaded Cerium on AC by impregnation method and assessed the adsorbent efficiency for DBT removal from model oils. Their report showed that Celoading on AC improved the adsorptive capacity and selectivity for DBT relative to when the AC was use alone. Furthermore, the improved performance of Ce-loading on AC was due to the variations in its surface chemistry. Yan et al. [27] conducted an experiment by synthesizing cerium oxide nanoparticles which were also loaded onto the surface of an activated carbon for SO₂ removal. They recorded a drastic improvement in the SO₂ sorption capacity compared to when the AC was used alone. SO₂ removal by activated carbon from palm kernel shell was demonstrated by Sumathi et al [28] where they impregnated the AC with Ce, Ni, V and Fe. Their results showed that activated carbon (AC) from palm shell modified with cerium nanoparticle gave the highest adsorption capacity, which may be due to the physicochemical characteristics of the admixed adsorbent and its catalytic activity.

Thousands of waste tea bags are generated on a daily basis especially in the heart of Lagos, Nigeria and are not properly disposed, hence, they constitute a serious challenge to the environment. However, despite the challenges, spent tea still has useful application as a precursor for the viable production of activated carbon for industrial purposes.

Works on admixed cerium nanoparticles with several activated carbons have been employed as adsorbents for DTB and BT removal from model fuels. However, works of admixed cerium and lanthanum oxide nanoparticles with activated carbon from spent tea have not been reported for the removal of sulphur compounds from a model oil. Therefore, the article aims at removing dibenzothiophene (DBT) and benzothiophene (BT) in a model oil using Ce/La oxide impregnation in spent tea activated carbon. The authors monitored the effectiveness of the prepared adsorbent and its importance in the refining industries. Characterization of the adsorbent, mechanisms, kinetics, thermodynamic properties isotherms were presented in the study.

2. MATERIALS AND METHOD

2.1 Reagent/adsorbate (Model Fuel)

Analytical grade chemicals were used for this study. 99.9 % pure Dibenzothiophene (C₁₂H₈S, 184.3 g/mol) and Benzothiophene (C₈H₆S, 134.20 g·mol⁻¹), as well as n-heptane by Sigma Aldrich were purchased. Sulphur concentration of 200 ppm (DBT and BT) in the liquid model fuel was used in this study.

2.2 Activated Carbon Preparation from Spent Lipton Tea

Activated carbon was obtained from spent Lipton tea in Nigeria. The spent tea was removed from the tea bag and then sundried for 24 h, after which it was immediately transferred to an oven and allowed to dry for 3 h at 105 °C. Carbonization of the spent

ISSN (Online):0493-2137

E-Publication: Online Open Access Vol: 56 Issue: 06:2023

DOI: 10.5281/zenodo.17275786

Lipton tea was conducted in a muffle furnace for 4 h at 400 °C at an initial heating rate of 10 °C/min for 20 minutes and was later cooled at 28 °C. Consequently, 10.0 grams of sieved (20 μ m) carbonized spent Lipton tea was treated with 10.0 mL of 0.5 M phosphoric acid, transferred into the furnace and carbonized at 300 °C under atmospheric condition while maintaining the same heating rate for an hour. The substrate was allowed to cool at room temperature, and thereafter washed with distilled water so as to remove any trace of phosphoric acid and allowed to dry in an oven overnight at 110 °C before it was finally kept in an air tight reagent bottle labeled as spent tea AC (SAC).

2.3 Synthesis of Cerium and Lanthanum Oxide Nanoparticles Via Sol Gel Method

Sol gel method was used for the nano-oxide synthesis. The cerium oxide nanoparticle was prepared by sol gel method following the method presented in ref. [4], while the La₂O₃ nanoparticle powder was obtained via sol-gel technique from micro-sized La₂O₃ powders, high-molecular weight polyethylene glycol (PEG) and 20% nitric acid as precursors. 10.0 grams of SAC was sonicated in 200 mL of deionized water and mixed with 50 mL C₂H₅OH while being stirred for 3 h. Ethylene glycol (30 mL) was added into the mixture which served as a linker between the metal ions and the surface-active sites of the SAC. 3 g each of the synthesized nanoparticle-powders were gently added simultaneously into the dispersed SAC. The mixture was maintained at a pH of 8 by the addition of sodium hydroxide and ammonia, while stirring continuously for 3 h. Furthermore, the system was heated at 80 °C for 5 h under continuous stirring until a precipitate was formed. The precipitate was filtered, washed and oven-dried at 105 °C for 24 h before being calcined in a furnace at 400 °C for 5 h. This was done for suitable adherence of the metal oxides on the SAC surface.

2.4 Adsorbent Characterization

The surface morphology of the adsorbent was examined using the JEOL-6610LV scanning electron microscope (SEM). The adsorbents' functional groups were characterized by the Perkin Spectrum 1000 Fourier transform infrared (FTIR) spectrophotometer within a bandwidth of 400 – 4000 cm⁻¹. The textures of the adsorbents were determined using the X-Max. JOEL-2000, USA high resolution transmission electron microscope (HRTEM). Characterization by the nitrogen adsorption-desorption technique (Brunauer-Emmett-Teller analysis) was conducted on the adsorbents' surface areas and porous structures.

2.5 Batch Adsorption Studies

Batch adsorption studies were conducted using SAC-Ce/La in 500-mL conical flasks having 30 mL of 200 ppm model oil. Adsorbent dosage ranging from 0.1-0.5 g was introduced into the flask; the flask containing the adsorbent and adsorbate was placed on a magnetic stirrer and agitated at room temperature until equilibrium was attained. During experimentation, at every period of time, aliquot samples were drawn using a syringe-filter which helped to take samples of the oil for onward detection of the oil's residual sulphur content using the sulphur chemiluminescence detector (SCD) integrated with a gas chromatograph.

ISSN (Online):0493-2137

E-Publication: Online Open Access Vol: 56 Issue: 06:2023

DOI: 10.5281/zenodo.17275786

The adsorbent efficiency was calculated using (1).

$$s = \frac{c_0 - c_e}{c_0} \times 100 \% \tag{1}$$

where s is the % sulphur adsorbed; C_e and Co represent the equilibrium and initial concentrations of sulphur in the model oil respectively. Thus qe (mg/g) can be expressed as:

$$q_e = \frac{V(C_O - C_e)}{m} \tag{2}$$

where $q_e(mg/g)$, can be expressed as the sulphur compounds adsorbed; V (L) is the fuel volume, and m (g) is the amount of sorbent.

2.6 Adsorbent Regeneration

One major challenge which poses environmental concern during desulphurization is the problem of disposal of the spent adsorbents.

Therefore, it is important to regenerate the adsorbent in order to ensure its recyclability, sustainability and reduced cost. The SAC-Ce/La regeneration was assessed after sorbent saturation with sulphur compounds.

The adsorbent recyclability was determined using the method of thermal regeneration. DTB and BT boiling points were determined to be 332.8 and 220 °C. For effective adsorption of the sulphur compounds present in the adsorbent, the adsorbent was treated at 350 °C for 2 h (350 °C was the optimum temperature for removing/vaporizing all the sulphur compounds, that adhered unto the surface of the adsorbent).

The regenerated adsorbent was further tested for its sulphur removal capacity in a batch mode.

2.7 Analysis of Experimental Data

Isotherm analysis, breakthrough curves, and kinetic models, were used to analyze the data obtained from the adsorption experiments. The parameters of pseudo first order (PFO) and pseudo second order (PSO) were also evaluated/calculated.

Also, the Freundlich and Langmuir isotherms as well as the thermodynamic parameters were determined. Table 1 contains the referred isotherms.

Table 1: Isotherms, their parameters and equations

Parameter	Equation
Langmuir Isotherm	$rac{C_e}{q_e} = rac{1}{K_L q_m} + rac{C_e}{q_m}$
Pseudo first order (PFO) model (linear form)	$In(q_e - q_t) = In q_e - k_1 t$
PSO	$\frac{t}{q_t} = \frac{t}{q_e} + \frac{1}{k_2 q_e^2}$
Freundlich Isotherm	$In q_e = In k_F + \frac{1}{n} In C_e$

ISSN (Online):0493-2137

E-Publication: Online Open Access Vol: 56 Issue: 06:2023 DOI: 10.5281/zenodo.17275786

3. RESULTS AND DISCUSSION

3.1 Characterization of the Adsorbent

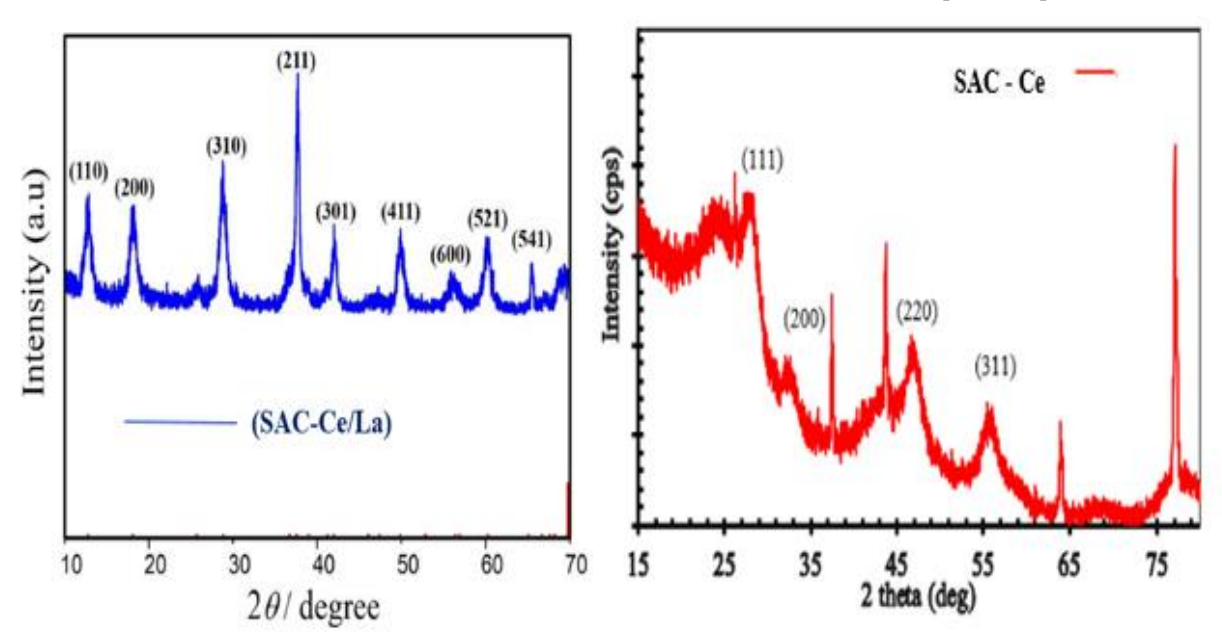
3.1.1 XRD Analysis of the Adsorbents

The XRD pattern for the SAC, SAC-Ce and SAC-Ce/La are illustrated in Figure 1. The peaks from the patterns show hexagonal meso-structures of the SAC-Ce and SAC-Ce/La. The XRD results display the crystalline phases of the two adsorbents. Each element possesses a distinctive pattern on exposure to the beam.

All adsorbents displayed broad diffraction peaks which is evidence of the presence of amorphous carbon. SAC-Ce/La displayed the transformation of the crystalline phase to an amorphous phase, thus indicating that the surface loading of La nano-oxide has impact on the mesoporous structure of SAC-Ce.

From figure 1, there are about eight peaks over hexagonal mesostructured related peaks; these peaks occur as a result of pore formation resulting from carbon decomposition along the direction of the activated carbon, thus indicating the semi-crystalline structure of the SAC-Ce/La.

Nevertheless, there are less intensities of SAC-Ce signals compared to SAC-Ce/La which is indicative of carbon surface replacement with La nano-oxide. The visibility of La diffraction patterns at 2θ are 36.5 (211), 28.7 (310), which suggest the presence of La nano-oxide in SAC-Ce; these results corroborate the works of refs. [29, 30].



ISSN (Online):0493-2137

E-Publication: Online Open Access Vol: 56 Issue: 06:2023

DOI: 10.5281/zenodo.17275786

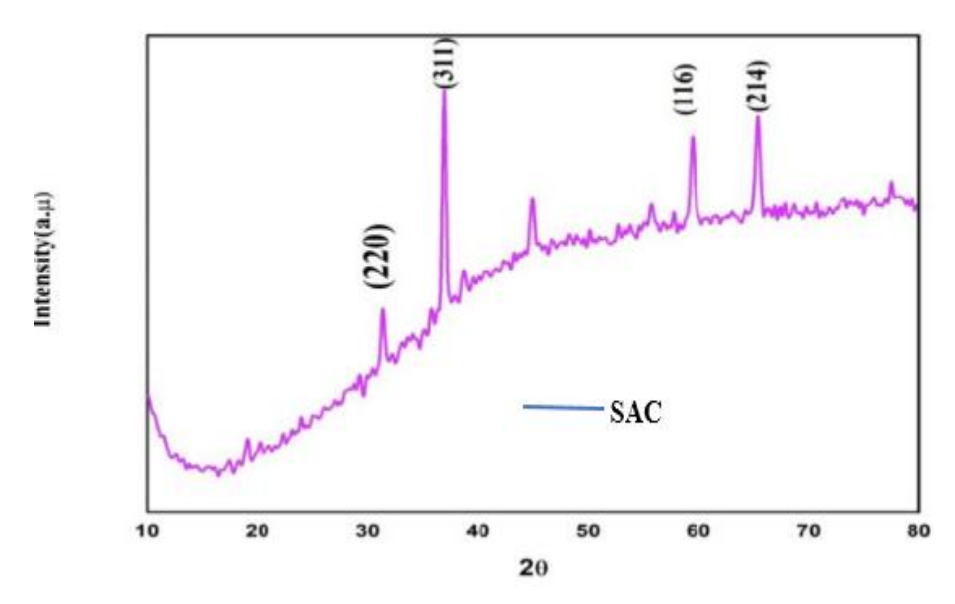


Figure 1: XRD pattern of (a) SAC-Ce/La (b) SAC-Ce (c) SAC

3.1.2 BET Results

The pore structures of the SAC-Ce and SAC-Ce/La, and their pore size distributions were analyzed using N_2 sorption (Figure 2). The IUPAC classification for the SAC-Ce and SAC-Ce/La curve is type-IV [31]. The isotherm has a strong upward trend at low pressures, which denotes the presence of microporous structures [32].

A hysteresis loop was observed at pressure of 0.80 - 1.0, thus confirming the presence of mesopores. Furthermore, low N_2 uptake was seen between 0.0 - 0.2, thus informing the presence of low micropores within the adsorbents [33].

The porous structural patterns of the adsorbents are presented in Table 2, with SAC, SAC-Ce and SAC-Ce/La having different surface areas of 191, 399.2 and 801 m²g⁻¹ respectively. The surface area of the SAC was very low due to the absence of the nano-oxides, however, with the inclusion/mixing of Ce oxide nanoparticle, the surface area as well as the pore volume tends to increase as presented in Table 2, thus, an inclusion of Ce/La nano-oxides in the SAC, displayed a marginal increase in the surface area/pore volume of the composite which is an indication of higher adsorption rate of BT and DBT, which corroborates the works of refs. [7, 25].

La oxide nanoparticle possesses some certain characteristics such as high surface-areato-volume ratio [11, 19] and good thermal and chemical stability [24], which are accountable for the high pore volume and surface area of the SAC-Ce/La.

Table 2: The textural parameters for SAC-Ce and SAC-Ce/La.

Adsorbent(s)	S _{BET} (m ² g ¹)	S _{micro} (m ² /g)	V _P (cm ³ / g)	V _{micro} (cm ³ / g)	V _{meso} (cm/g)
SAC	191.8	99.4	0.68	0.09	0.19
SAC-Ce	399.2	171.9	1.02	0.11	0.41
SAC-Ce/La	801.6	316.1	1.12	0.17	1.16

E-Publication: Online Open Access Vol: 56 Issue: 06:2023

DOI: 10.5281/zenodo.17275786

3.3.1 Pore Size and Pore Structure Distribution

By analyzing the pore size distributions and micro and mesopore volumes shown in Fig. 2, the degree of micro-porosity and the establishment of the pore structure of the various adsorbents were assessed. By considering that layers accumulate on the pore wall until the pore is fully filled, Fig. 2 is an illustration of the measured the volume of the pores. This characteristic is as a result of the inherent surface areas of the adsorbents. The SAC, SAC-Ce, and SAC-Ce/La carbons' pores are primarily found in the micropore region, having a peak at 1.2 nm. It can be shown from Tables 2 that SAC-Ce/La had the maximum BET surface area and micropore volume, thus indicating that the micro-pores constitute the most pores on the surface. Thus, a well-ordered structure is expected to be developed in the SAC-Ce/La which leads to high adsorption rates. Textural analysis of the textural characteristics of the modified and unmodified adsorbents were investigated using N₂ adsorption-desorption isotherms. All isotherms are type IV profiles, which is typical of mesoporous materials with obvious inflections under high relative pressure.

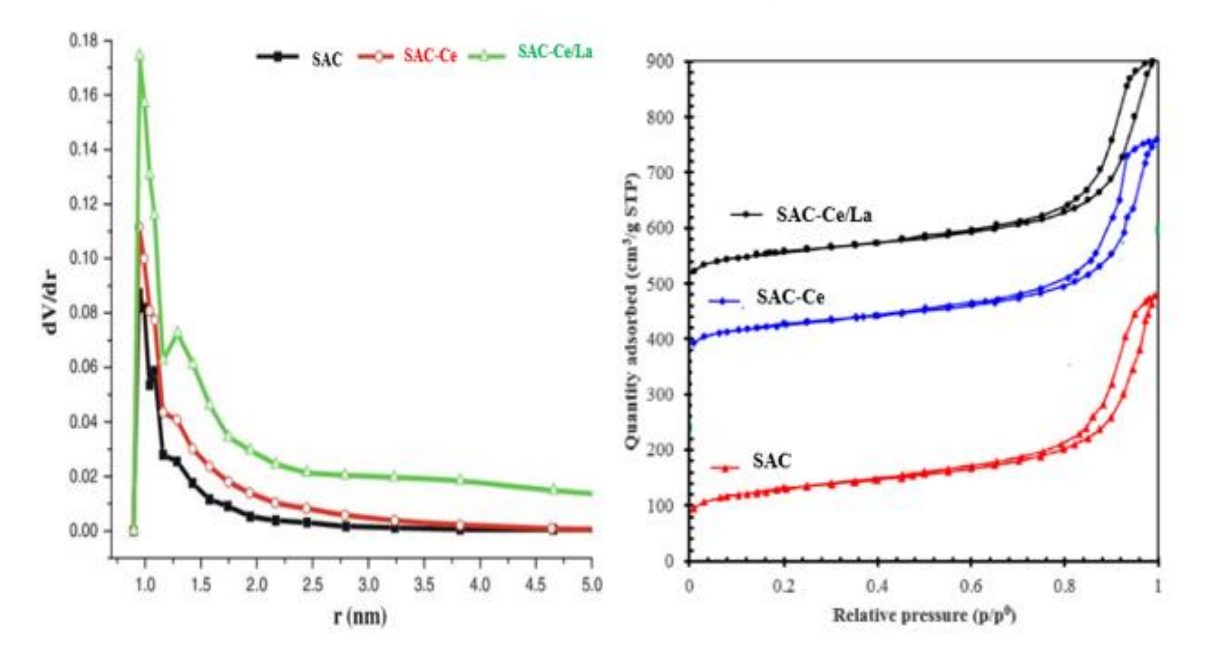


Figure 2: Pore size distribution of SAC, SAC-Ce and SAC-Ce/La

3.1.3 SEM Characterization

The SEM of the adsorbents are presented in Figure 3. The adsorbents' morphologies are displayed as SEM images based on the surface characteristics of the adsorbents. The obtained results are in-line with the BET, XRD and FT-IR. The images show the presence of activated carbon- nanoparticles, thus demonstrating a homogeneous metal oxide loading on the site of the SAC. The white deposits on the SEM images signify the presence of nanoparticles on the SAC (Figure 3a). Furthermore, the addition of lanthanum nanoparticles unto SAC-Ce, result in higher removal of sulphur compounds

ISSN (Online):0493-2137

E-Publication: Online Open Access Vol: 56 Issue: 06:2023

DOI: 10.5281/zenodo.17275786

(Figure 3b). These nanoparticles highly contribute to the chemisorption of BT and DBT through sulphur/metal interaction [33-34].

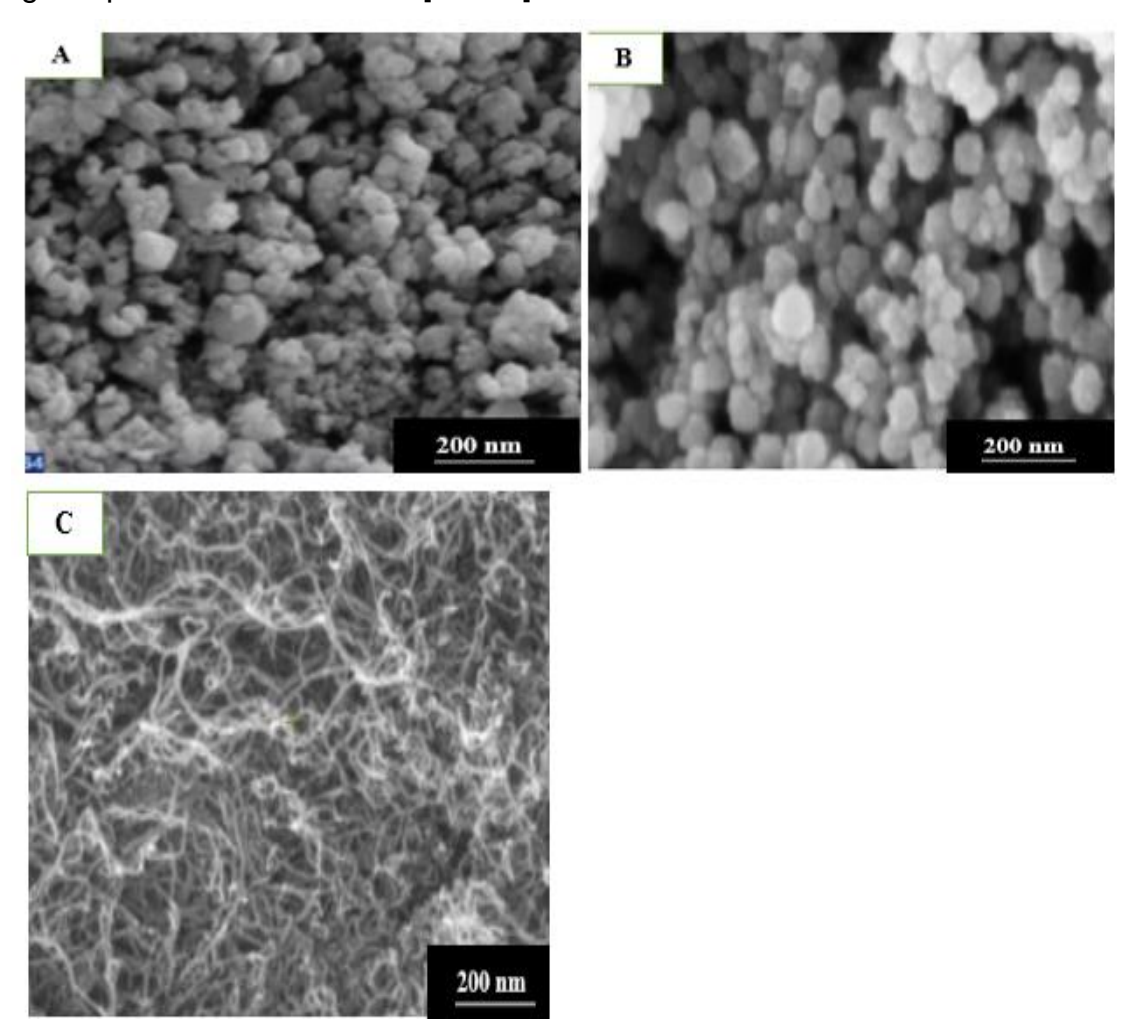


Figure 3: (a) SAC-Ce/La (b) SAC-Ce (C) SAC

3.1.4 Transmission Electron Microscopes (TEM) Characterization

The TEM images of SAC, SAC-Ce and SAC-Ce/La adsorbents are presented in Fig. 4. The finger-like, pores, and structures obtained from the micrographs are as seen on the adsorbents' (SAC-Ce and SAC-Ce/La's) surfaces.

All adsorbents are uneven and irregular. The SAC-Ce/La surface appears to be rougher and different when compared to that of SAC-Ce due to La nano-oxide addition on the SAC-Ce surface, which may be accountable for the higher adsorption capacity of SAC-Ce/La.

The pores on the surface of the adsorbent pose less resistance to the adsorbed molecules, thus, allowing for the easy diffusion of the adsorbate from the model fuel onto the surface of the adsorbent; this corroborates the findings of ref. [35].

ISSN (Online):0493-2137

E-Publication: Online Open Access Vol: 56 Issue: 06:2023

DOI: 10.5281/zenodo.17275786

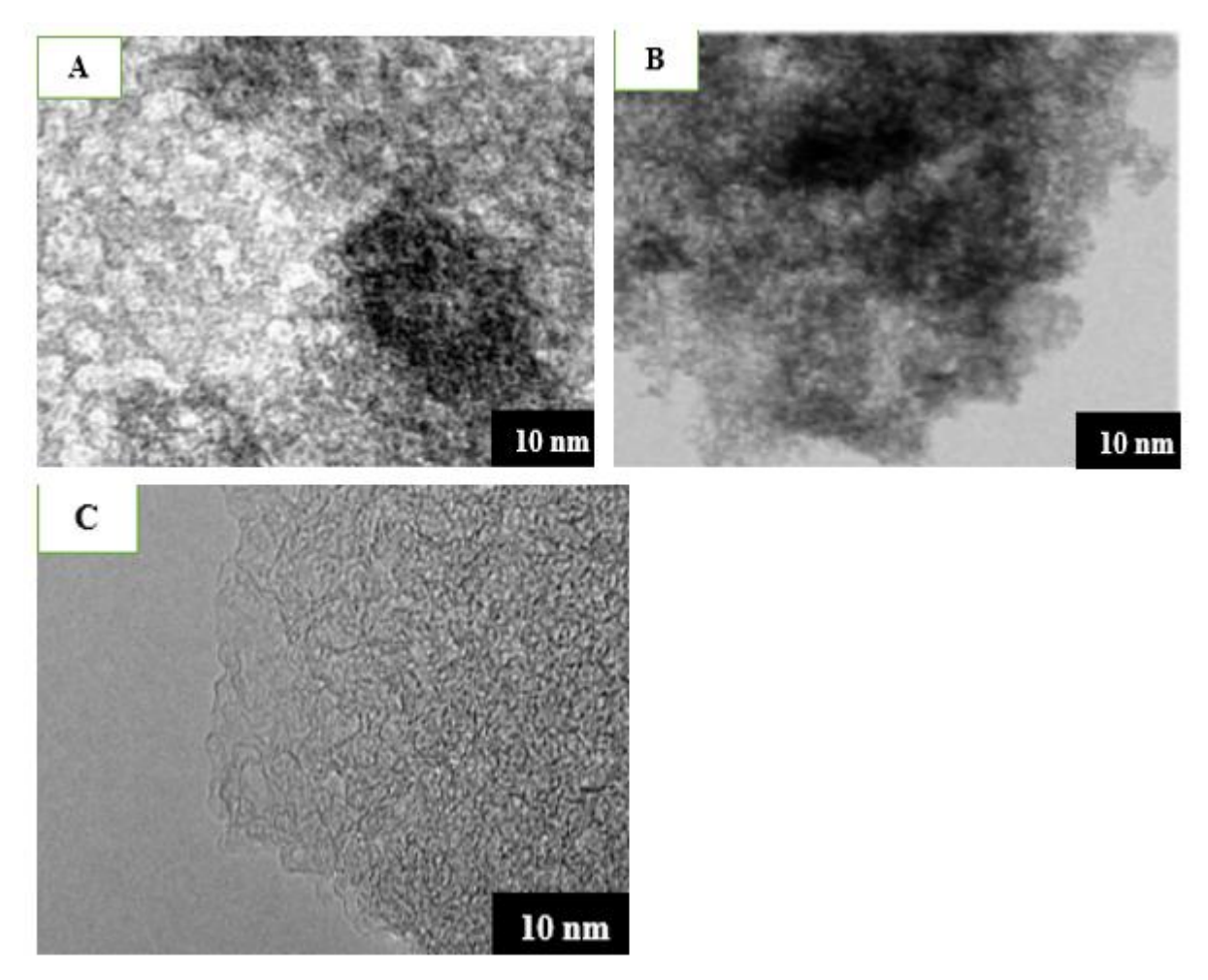


Figure 4: TEM images of (a) SAC-Ce/La (b) SAC-Ce (c) SAC

3.1.5 FT-IR Characterization

Fig. 5 presents the adsorbents' FT-IR spectra which helps to identify the functional groups that are present in the adsorbents and to observe any resemblance in the intensities of every functional group present. For the SAC, SAC-Ce and SAC-Ce/La, the FT-IR profiles are indicative of the asymmetric occurrence of the Si–O–Si bond between 884/cm – 1738/cm, 895 - 3317/cm and 900/cm – 3500/cm respectively [22]. Impregnating La nano-oxide unto SAC-Ce results in the fading of sites that are inactive due to the ability of La ions to substitute the hydrogen ions of the vibrations that are inherent in the Si–OH. Therefore, there is a possibility of allotting the weak bands to Ce-S bond vibrations in the BT and DBT (adsorbed compound) [11]. The peaks observed at 1019 and 1020/cm are related to the C-O-C stretching and CO(-COH) stretching of SAC-Ce and SAC-Ce/La [30]. The peak found at 895 and 900/cm probably corresponds to the S-N stretching mode which is typical of Si–OH. There exists a reaction of sulphur atom with π -complexion with the adsorbents after the adsorption of BT and DBT. Finally, the C=C vibrations in the adsorbed sulphur would result in weak bands [27].

ISSN (Online):0493-2137

E-Publication: Online Open Access Vol: 56 Issue: 06:2023

DOI: 10.5281/zenodo.17275786

The alteration of the SAC-Ce/La surface oxygen-containing functional groups (-COOH, -C=O, and -C-O) may change its physical and chemical characteristics, which may affect its desulphurization activity [32]. These FT-IR peaks confirm the presence of amorphous carbon which correspond to higher intensities of the synthesized SAC-Ce/La. This also justifies the results of the SEM, BET and XRD.

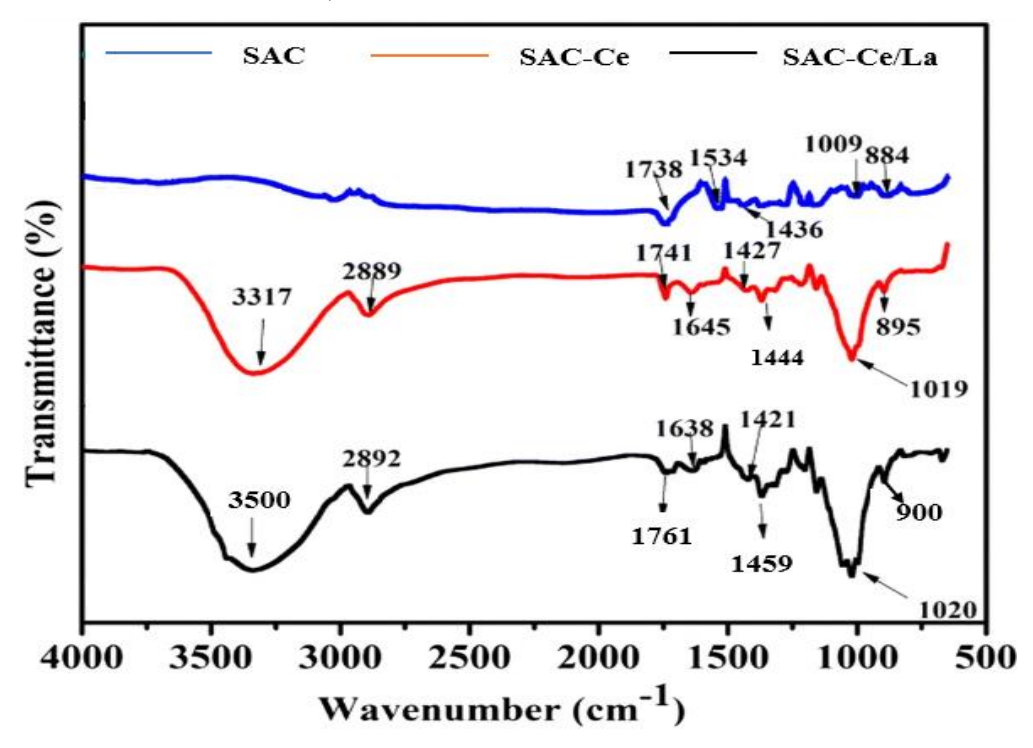


Figure 5: FT-IR Spectrum of (a) SAC-Ce/La (b) SAC-Ce (c) SAC

3.2 Adsorbent Removal of Sulphur Compounds

Batch adsorption study was conducted on the removal of sulphur by the SAC-Ce/La adsorbents. The reaction process was rapid at 5 minutes. Although, equilibrium was achieved at 10 minutes (Figure 6), the SAC-Ce/La adsorbent performed excellently owing to its high pore volume and large surface area, thus confirming the hypothesis that altering/enhancing AC surface with nanoparticles increases its adsorptive capacity as well as its selectivity for sulphur compounds i.e., La/ Ce nano-oxides interaction was responsible for the adsorbent's high efficiency in removing compounds of sulphur (DBT/BT) compared to the SAC bearing cerium nanoparticle on its surface[22]. La nano-oxide may have indirect consequence on the solution, thus creating an acidic site needed for the adsorption of the base. BT and DTB compounds allow/prefer Lewis bases, thus permitting interactions with acidic sites. Thus, Ce/La nano-oxides on SAC is highly efficient in adsorbing the sulphur compounds of BT and DBT. The excellent performance of SAC-Ce/La in removing DBT/BT may be due to the adsorbent having additional π -complexions, thus providing additional interactions on the adsorbent's' active sites [8, 28, 33].

ISSN (Online):0493-2137

E-Publication: Online Open Access Vol: 56 Issue: 06:2023

DOI: 10.5281/zenodo.17275786

Therefore, the interactions that occurred on the delocalized π -electrons in the interior of the aromatic ring of dibenzothiophene and the electron-rich region on the SAC-Ce/La is very important in the adsorption process.

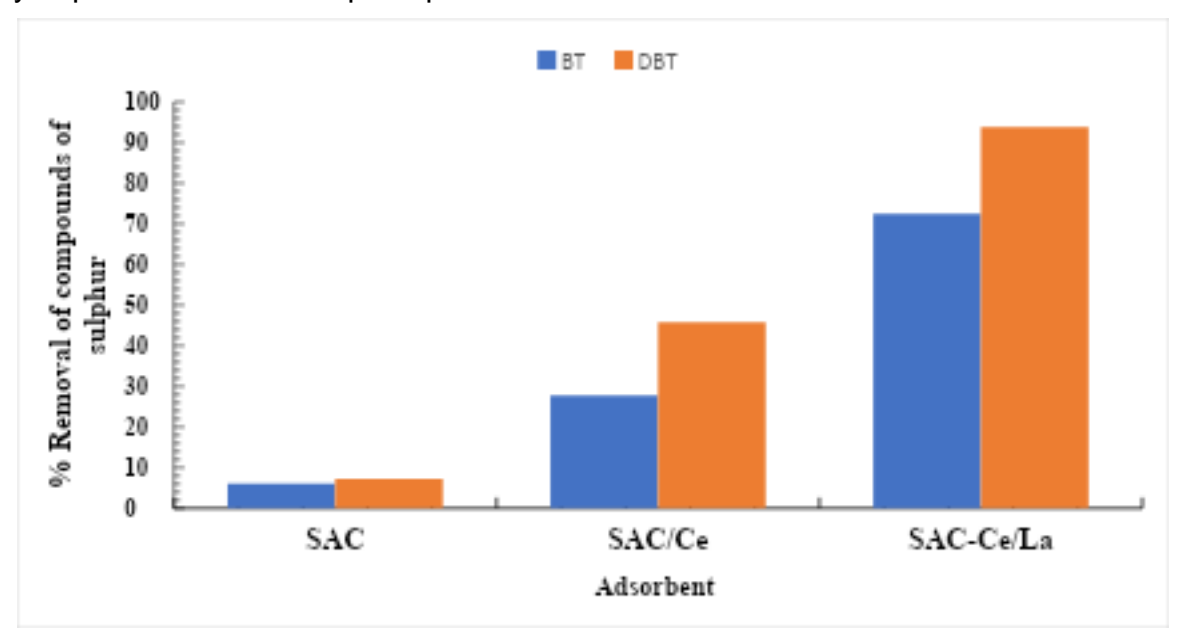


Figure 6: % adsorption of BT, DBT by SAC, SAC/Ce and SAC-Ce/La

The NH₃-TPD spectra of the SAC, SAC-Ce, and SAC-Ce/La adsorbents are displayed in Figure 7. The area under NH₃ the desorption curve was used to evaluate the acidity of the adsorbents.

For majority of the time, the acid sites were categorized based on the desorption temperature by the weak acid sites being those formed within temperatures 25-220 °C, the medium acid sites were formed at a temperature of 220-400 °C, while the strong acid sites were those formed at temperatures above 400 °C [33].

The increase in active sites at high temperatures is due to NH₃ desorption from strong acid sites, whereas the peak between 206 and 268 °C may be due to NH₃ desorption from weak acid sites [34].

Weak and medium acid sites were indicated by a desorption peak in the range of 100 – 360 °C in the NH₃-TPD spectrum of SAC and SAC-Ce. Among the adsorbents, the SAC-Ce/La had the highest level of acidity, which may have been caused by the larger loading of hetero-poly acids on the adsorbent.

The reduced (DBT/BT) content of the samples is responsible for the disappearance of the strong acid sites in the SAC-Ce/La adsorbent [39].

E-Publication: Online Open Access Vol: 56 Issue: 06:2023

DOI: 10.5281/zenodo.17275786

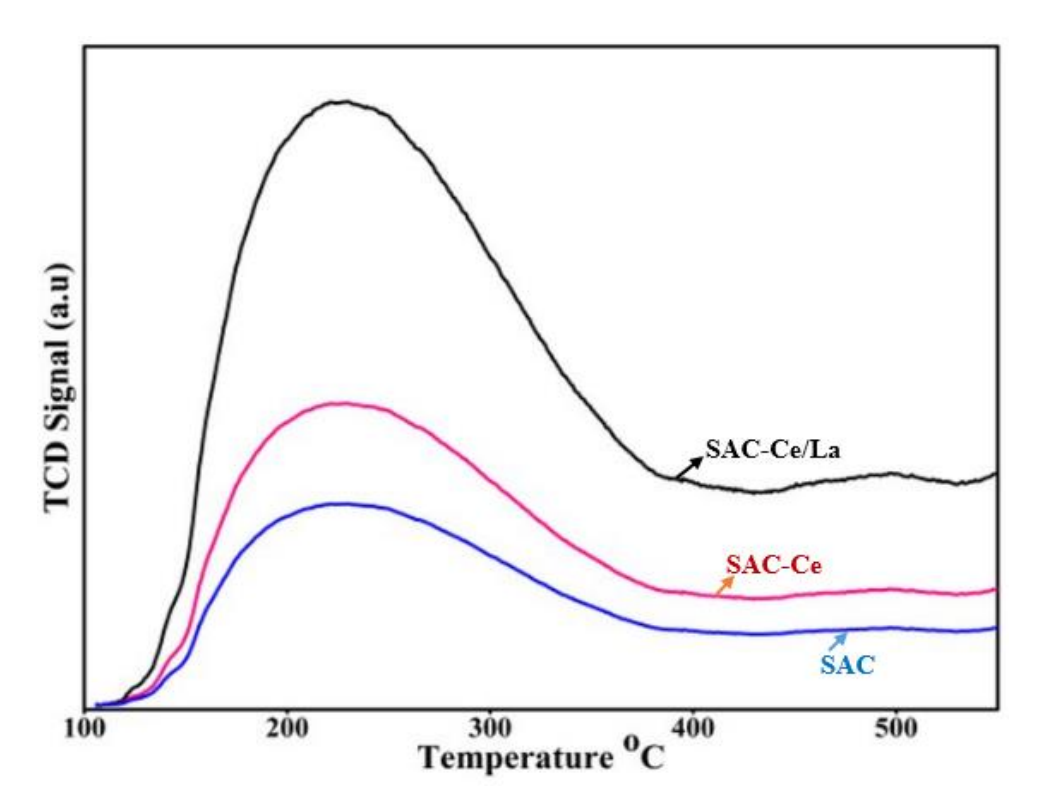


Figure 7: NH₃-TPD spectra of SAC, SAC-Ce and SAC-Ce/La adsorbent

3.3 Effect of Contact Time

Figure 8 presents the effect of contact time on the sulphur degradation in benzothiophene and dibenzothiophene from the model oil at room temperature with SAC-Ce/La. After 5 minutes, the adsorption process was relatively fast. The batch adsorption method attained equilibrium in roughly 10 minutes, thus demonstrating a fast adsorption process. Between 10 and 14 minutes, the BT and DBT absorption were determined to be 9.3 mg/g and 13.2 mg/g. The SAC-Ce/La's initial quick adsorbate uptake capacity occurs as a result the availability of vacant sites at the preliminary phase, followed by the resistance offered with respect to occupying the remaining vacant sites as a result of the increased concentration gradient that occurred between the molecules of the S- compound in solution and that of the adsorbent (SAC-Ce/La) [11, 24, 35]. Furthermore, S-compounds are adsorbed into the pores from the model oil which was almost saturated with the BT/DBT at the initial adsorption stage. Thereafter, the molecules of the BT/DBT diffused at a deeper and faster rate into the pores of the adsorbent, thus experiencing a higher resistance, which then led to the decreased DBT/BT-sorption rate that eventually approaches saturation. The BT/DTB were substantially sufficient to be packed on the adsorbent's surface, thus limiting them from passing through the adsorbent's pores easily [32,35]. The diffusion coefficient of the adsorbent in the solid/bulk phase, the size of SAC-Ce/La molecules, degrees of mixing in the batch experiment, the analyte concentration and the adsorbent's affinity for the analytes all restrict the rate and quantity of DBT/BT absorbed by the SAC-Ce/La. By extending the contact period, the number of accessible

E-Publication: Online Open Access Vol: 56 Issue: 06:2023

DOI: 10.5281/zenodo.17275786

adsorption sites reduced as the amount of DBT/BT adsorbed increased [36]. After a while, the S-compounds must go deeper and deeper into the micropores, thus encountering significantly higher resistance, which subsequently resulted in lowering the adsorption rate over time. For BT/DBT, SAC-Ce/La gave a greater adsorption capacity of 31.9 mg/g, whereas the SAC-Ce and SAC gave lower capacities of 20.5 mg/g and 10.0 mg/g. The enhancement of SAC-Ce/La for the adsorption of BT/DBT from the model oil may have occurred as a result of the presence of more acidic sorption sites that are present on the surface of AC, thus resulting in a higher intensity of BT/DBT interaction with SAC-Ce/La. Thiophenic compounds interact with metal oxides either by donating a lone pair of electrons from sulphur, thus establishing a direct S-M σ -bond or via delocalization of π -electrons of the aromatic ring which in turn forms a π -type complex with the metals. Ce exist as Ce²⁺ when in contact with air due to its poor reduction potential [8]. The oxidized Ce may form a complex with benzothiophene and dibenzothiophene via S- Ce - σ -bond, thus resulting in significant BT/DBT adsorption on the SAC surface [37].

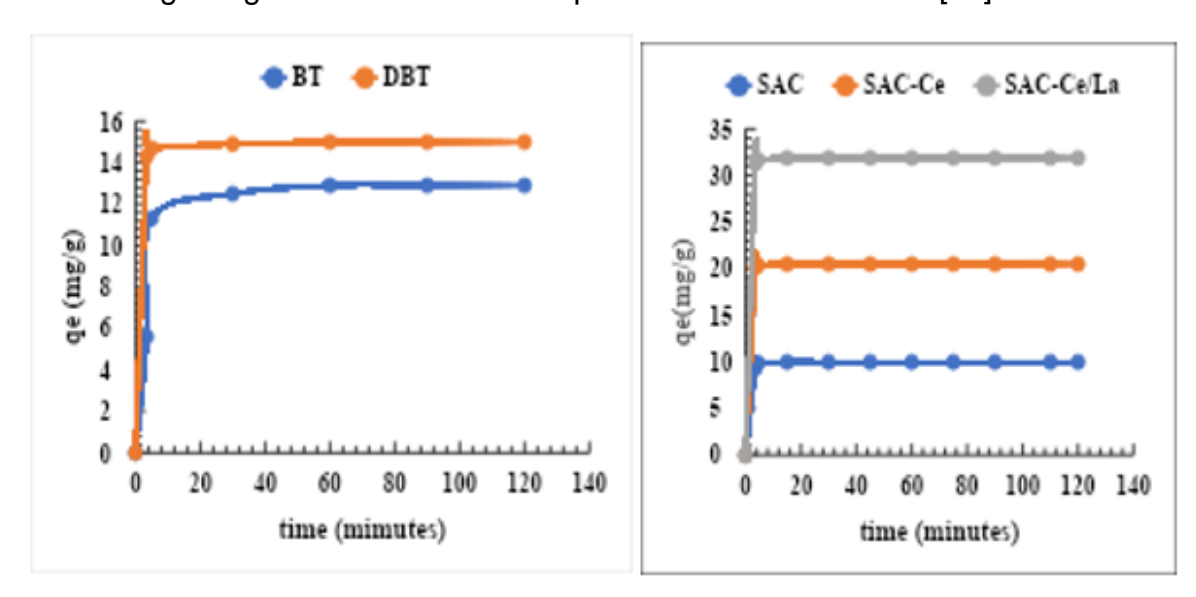


Figure 8: (a) Effect of contact time on sulphur adsorption by SAC-Ce/La in batch mode from BT and DBT. (b) Effect of contact time on the three adsorbents used for BT/DBT removal

3.4 Effect of Adsorption Dosage

Figure 9 illustrates the effect of adsorbent-dosage on the DBT/BT compounds. The dosage (0.10-0.50~g) was administered with a set of initial concentrations of DBT and BT of 50 ppm in 25 mL of the model oil at 28 °C since identifying the optimal adsorbent dosage is a significant parameter in an adsorption process. As the adsorbent dosage increased, the adsorption of the adsorbate improved as a result of the availability of additional sorbent surface area, which increased the number of adsorption sites in the medium. Another possibility might be an increase in the driving force imposed by

ISSN (Online):0493-2137

E-Publication: Online Open Access Vol: 56 Issue: 06:2023

DOI: 10.5281/zenodo.17275786

the concentration gradient that occurred between the adsorbent's surface and bulk solution [11].

Irrespective of the adsorbent-dosage, the percent adsorption of DBT/BT was > 85%. As a result, for all doses tested, the percent removal of BT was 77. The acid-base interaction between DBT/BT is also another enhancement parameter that stimulated such results.

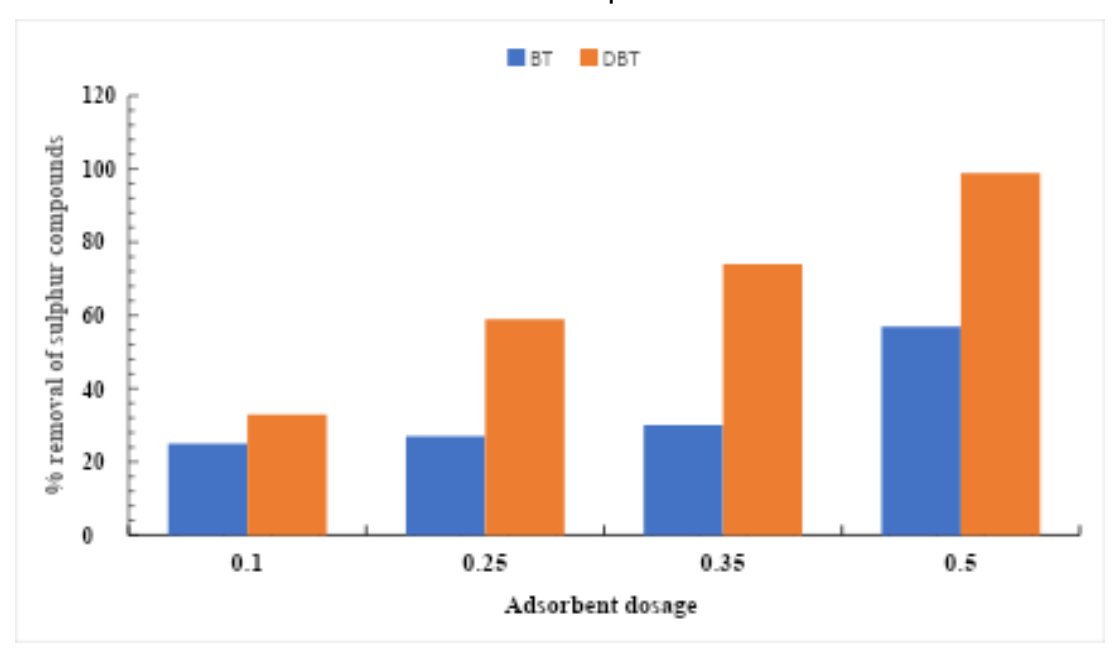


Figure 9: Effect of SAC-Ce/La dosage on BT/DBT

3.5 Breakthrough Pattern/Curve

In column mode, the performance of SAC-Ce/La was studied further (continuous flow mode). The concentration of total DBT/BT normalized by the feed/total DBT/BT concentration (Ct/C_0) was plotted against the cumulative time which yielded a breakthrough curve.

The curve is shown in Figure 10, and DBT removal was higher compared to DT as seen in the breakthrough after 50 minutes. Nevertheless, even after 240 minutes, the DBT concentration did not return to its previous level, thus indicating that the DBT adsorption continued completely throughout the column investigations.

After 25 minutes of adsorption, the breakthrough of BT adsorption was achieved, and after 60 minutes of adsorption, it was practically back to where it was before the breakthrough. After reaching the saturation point, C/C_0 values slightly exceeded unity as seen in Figure 10.

This is due to the partial reversibility of the adsorption over SAC-Ce/La compared to the successive break through during adsorption of the compounds, thus resulting in the partial substitution of compounds with the lower affinity for higher adsorptive compounds [38].

ISSN (Online):0493-2137

E-Publication: Online Open Access Vol: 56 Issue: 06:2023

DOI: 10.5281/zenodo.17275786

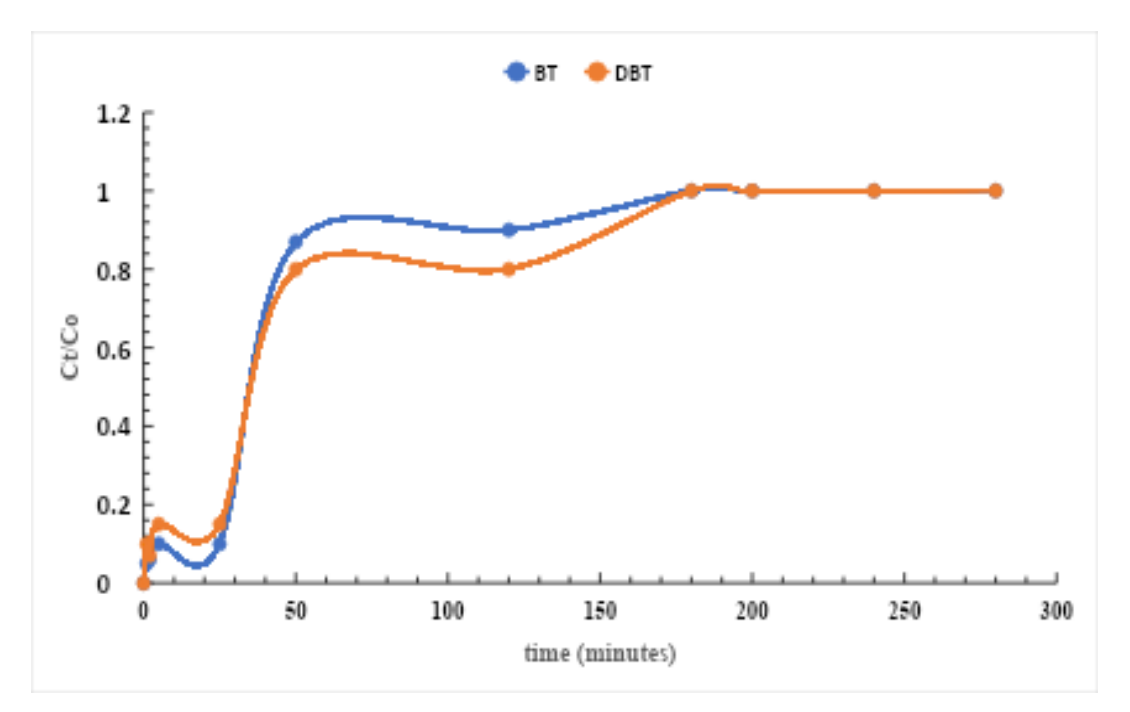


Figure 10: Breakthrough curve for BT and DBT using SAC-Ce/La

3.6 Adsorption Isotherms of BT/DBT

An adsorption isotherm is defined by a set of parameters that describe the adsorbent's surface characteristics and affinity which can be used to examine the adsorbent's adsorptive capabilities for different contaminants. The Freundlich and Langmuir isotherms were studied using the SAC-Ce/La adsorbent for the removal of BT and DBT from the model oil [15, 18, 21]. The Langmuir model assumes that the maximum adsorption corresponds to a saturated monolayer of solute on the surface of the adsorbent.

The Freundlich isotherm (Table 1) describes a multilayer adsorption or a heterogeneous process. The "n" values indicate the adsorption process's favorability, with values of n > 1 under favourable conditions [24]. The Freundlich isotherm constants, K_F and n are calculated using the slope/intercept. The adsorption of DBT increases as the adsorbate concentration rises. This could be largely attributable to the model oil's hydrophobic nature, which is adsorbed by SAC-Ce/La, and in turn results in the removal of BT/DBT from model oil. Nevertheless, at lower concentrations, q_e increased rapidly, whereas at higher Ce values, the q_e increased gradually.

The isotherms' linearity further validates the BT/DBT's competitive adsorption for the adsorbents' adsorption sites [17]. The adsorption of dibenzothiophene and benzothiophene on SAC-Ce/La is promising (Figure 11). The R² values for BT/DBT in the Freundlich isotherm as shown in Table 2 reveals that the plot is more linear than that of the Langmuir isotherm. Furthermore, the R² experimental data fits well with the Freundlich isotherm model.

ISSN (Online):0493-2137

E-Publication: Online Open Access Vol: 56 Issue: 06:2023

DOI: 10.5281/zenodo.17275786

Table 2: Langmuir and Freundlich isotherms data from SAC-Ce/La adsorbent

Sulphur compound analyzed	Langmuir isotherm variable				Freundlich isotherm variable		
	q _m (mg. g- ¹)	K _L (L/mg)	R∟	R ²	n	R ²	K _F
BT	51.8	0.052	0.511	0.9511	2.8	2.7	0.9995
DBT	56.2	0.049	0.257	0.9892	1.3	1.2	0.9998

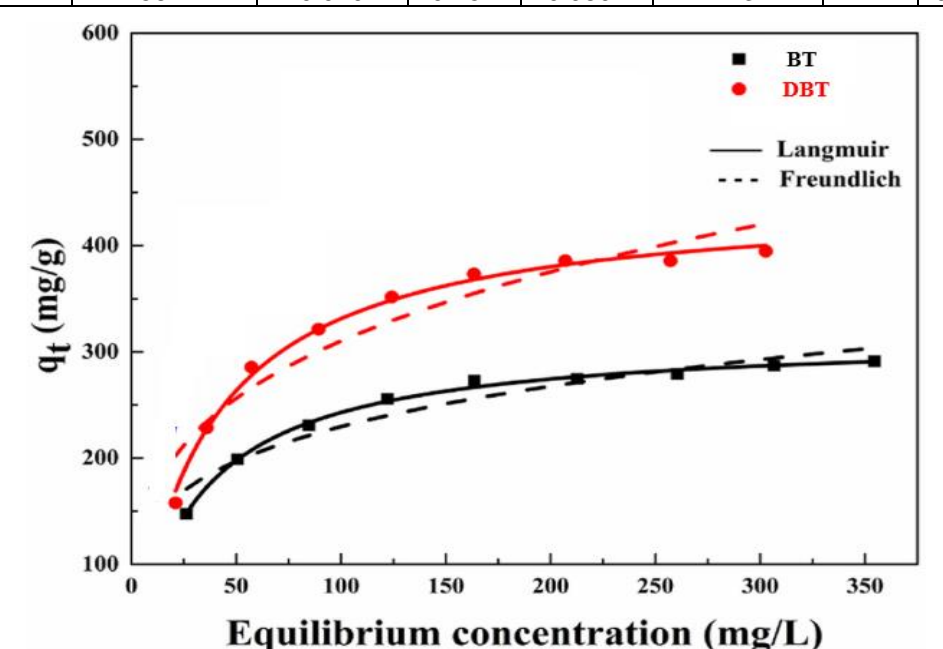


Figure 11: Langmuir and Freundlich isotherm for the adsorption of DBT and BT onto SAC-Ce/La adsorbents

3.7 Kinetic Model

The interaction and sorption mechanism between SAC-Ce/La and the analytes are revealed by the adsorption kinetics (DBT, and BT). To explain the adsorption mechanism, the linear representations of PFO and PSO were used. Estimated correlation coefficient (R²) values were used to assess the relationship between the kinetic model and experimental data. The PFO and PSO constants are represented by k₁ and k₂. The PFO kinetic model tool estimates the adsorbent's (SAC-Ce/La's) adsorption capacity towards the analyte molecules and thus justifies the adsorption process at an early stage. The model is shown in its linear form in Table 1.

For all DBT/BT compounds, the discrepancy between the experimental and calculated values demonstrates that the adsorption kinetics obeyed the PFO model to an extent. Furthermore, when compared to the PSO kinetic model, the results calculated from the correlations (R²) of BT/DBT (Figure 12) were lower, thus indicating that the process is not the first order type. The results showed that the adsorption of BT/DBT on the SAC-Ce/La surface somewhat deviates from the PFO model. The PSO kinetic model better-defines the adsorption capacity by assuming chemisorption aided by valence forces which bring

E-Publication: Online Open Access Vol: 56 Issue: 06:2023

DOI: 10.5281/zenodo.17275786

about the exchange of electrons as the rate limiting step. As a result, the obtained data were fitted, which affirms the linearity of the PSO model at varied contact times between the adsorbent and analytes, as shown in Table 3. The calculated and experimental q_e values of BT/DBT are in line with the PSO'as informed by the higher/estimated $\rm R^2$. The study indicated that the chemisorption mechanism, in which covalent bonds/electrons are formed between the analytes and adsorbent's surface, controls the adsorption of the sulphur compounds onto SAC-Ce/La.

Table 3: Kinetic models for BT/DBT removal from model oil onto SAC-Ce/La

Model	Kinetic parameters	Compound		
		BT	DBT	
PFO	q_e , exp (mg/g)	8.08	17.74	
	q_e , cal. (mg/g)	3.06	4.69	
	$k_1(min^{-1})$	0.035	0.067	
	R ²	0.9365	0.9661	
PSO	q_e , cal. (mg/g)	7.79	16.99	
	$k_2(\frac{g}{mg}.min^{-1})$	0.099	0.405	
	R ²	0.9994	0.9989	

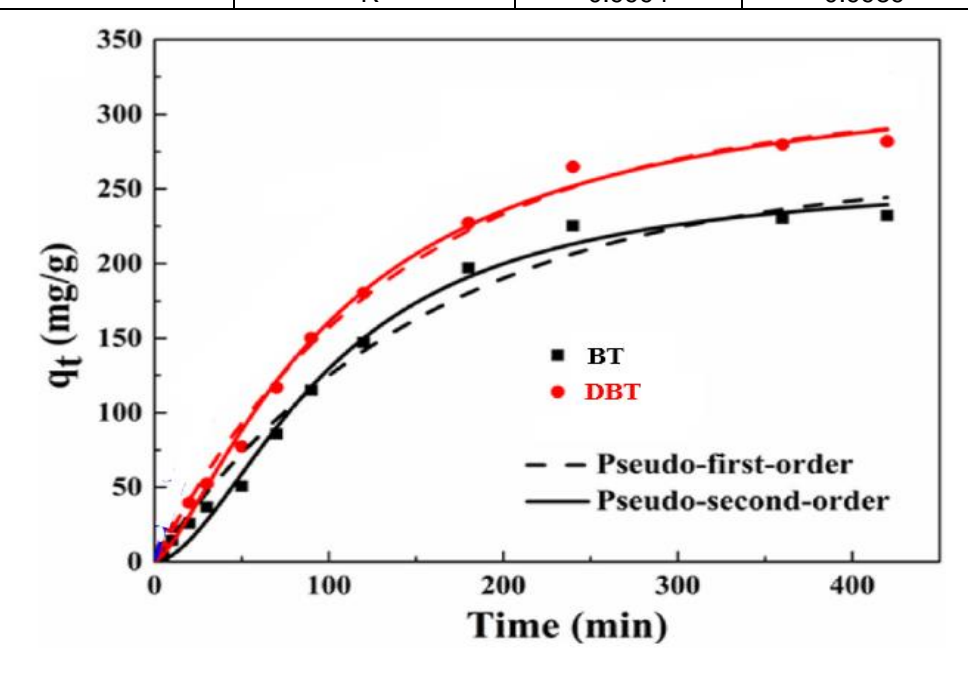


Figure 12: Kinetic model on SAC-Ce/La Adsorption

3.8 Reusability

The disposal and regeneration of wasted adsorbents are two main challenges with the use of adsorbents in ADS. Ultrasound, thermal, and solvent regeneration procedures are now being used to regenerate ACs [29, 37]. In this study, the thermal regeneration approach was used. The SAC-Ce/La was re-used for subsequent adsorption, and the

ISSN (Online):0493-2137

E-Publication: Online Open Access Vol: 56 Issue: 06:2023

DOI: 10.5281/zenodo.17275786

step was repeated 5 times. The adsorbent's reusability is a key factor in industrial applications. Calcination in air at 400 °C for 12 h, after which it underwent activation/autoreduction in helium flowing for 18 h at 450 °C, was used to regenerate the used adsorbent. In a 5-cycle adsorption—regeneration procedure, the adsorbent still maintained its reusability above 80%. After the first regeneration (Figure 13), there was a modest loss in adsorption capacity, followed by a considerable reduction after 5 regeneration cycles. The deposition of degraded byproducts of the adsorbent-adsorbate interactions on the adsorbent's surface, caused a reduction in the adsorbent's adsorptive ability.

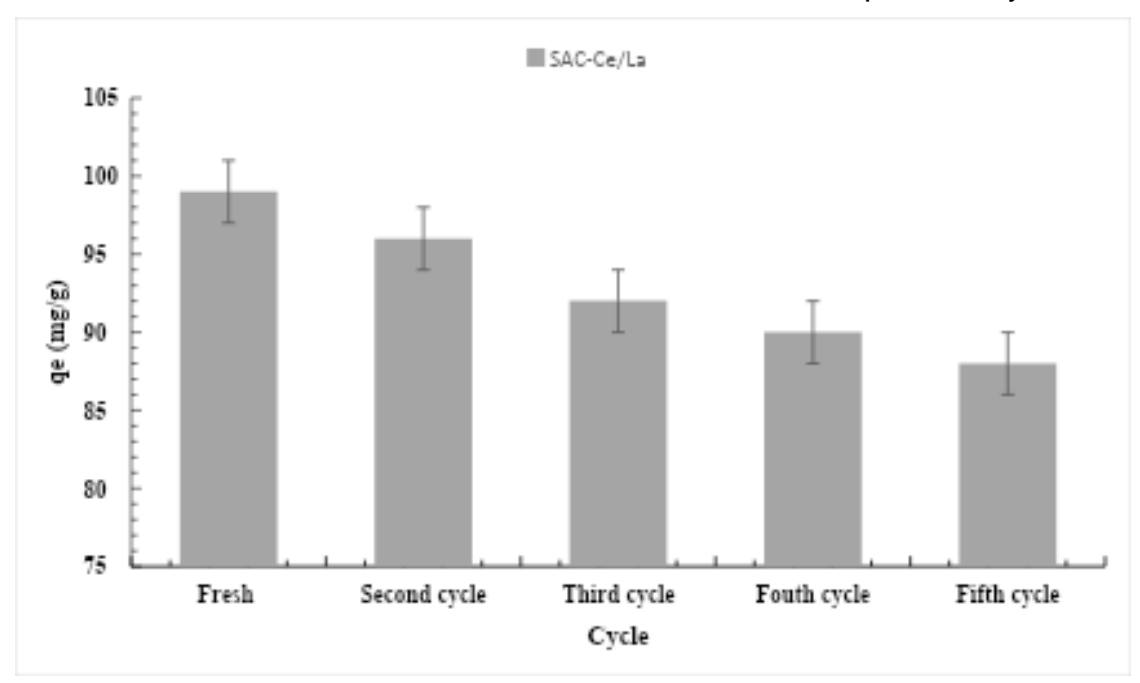


Figure 13: Removal efficiency at each cycle

Various comparisons of the adsorption capacities of the adsorbent for S-compound removal from a model oil as reported by some authors are presented in Table 4.

Table 4: Adsorption capacities of DBT removal from model oil as reported by some researchers

Model oil	Adsorbent	Adsorption capacity	Ref.
n-Hexane	Modified Zeolite	109	[6]
n-Heptane	Activated carbon treated with steam at 900 °C then washed by H ₂ SO ₄	47.1	[13]
n-Heptane	AC-MnO ₂	43.2	[19]
n-Hexane	Thermally treated AC fiber,	14.0	[29]
n-Heptane	Acid activated carbon	13.9	[31]
n-Docane/toluene	AC-Cu Y zeolite	5.0	[35]
n-Hexane	Thermally treated AC fiber and modified Cu copper cation	19.0	[38] This study
n-heptane	SAC-Ce/La	56.2	Triis study

E-Publication: Online Open Access Vol: 56 Issue: 06:2023 DOI: 10.5281/zenodo.17275786

3.4.4 Reaction Mechanism

In ADS, SAC-Ce/La was used to selectively degrade sulphur compounds (BT/DBT) from n-hexane. ADS is a fairly easy procedure that requires little energy and can be carried out in batch/column mode. The BT/DBT were preferentially held by the SAC-Ce/La during the feed's contact with it. The desulphurized feed is separated, and the feed is recycled to achieve further desulphurization until the sulphur breakthrough occurs. The adsorbent material's properties, such as its selectivity, adsorption capacity, regeneration capability, mechanical stability and the process conditions are what determine how effective the process is [39]. For the desulphurization of model oil, SAC-Ce/La has demonstrated a promising and improved efficiency over SAC without La/Ce. The adsorbent's structure has a significant impact on the action of the SAC-Ce/La. DBT/BT compounds are bound to the adsorbent as a result of a chemical reaction through chemical bonding [40]. In this process, the sulphur atom is attached to the adsorbent as sulphide, thus changing the character of DBT/BT primarily, by breakdown. The SAC-Ce/La regeneration cannot be accomplished through physical procedures since DBT/BT is chemically bonded to the adsorbent. The DBT/BT may be removed as H₂S or sulphur oxides during the regeneration of the adsorbent [41] as described in Figure 14.

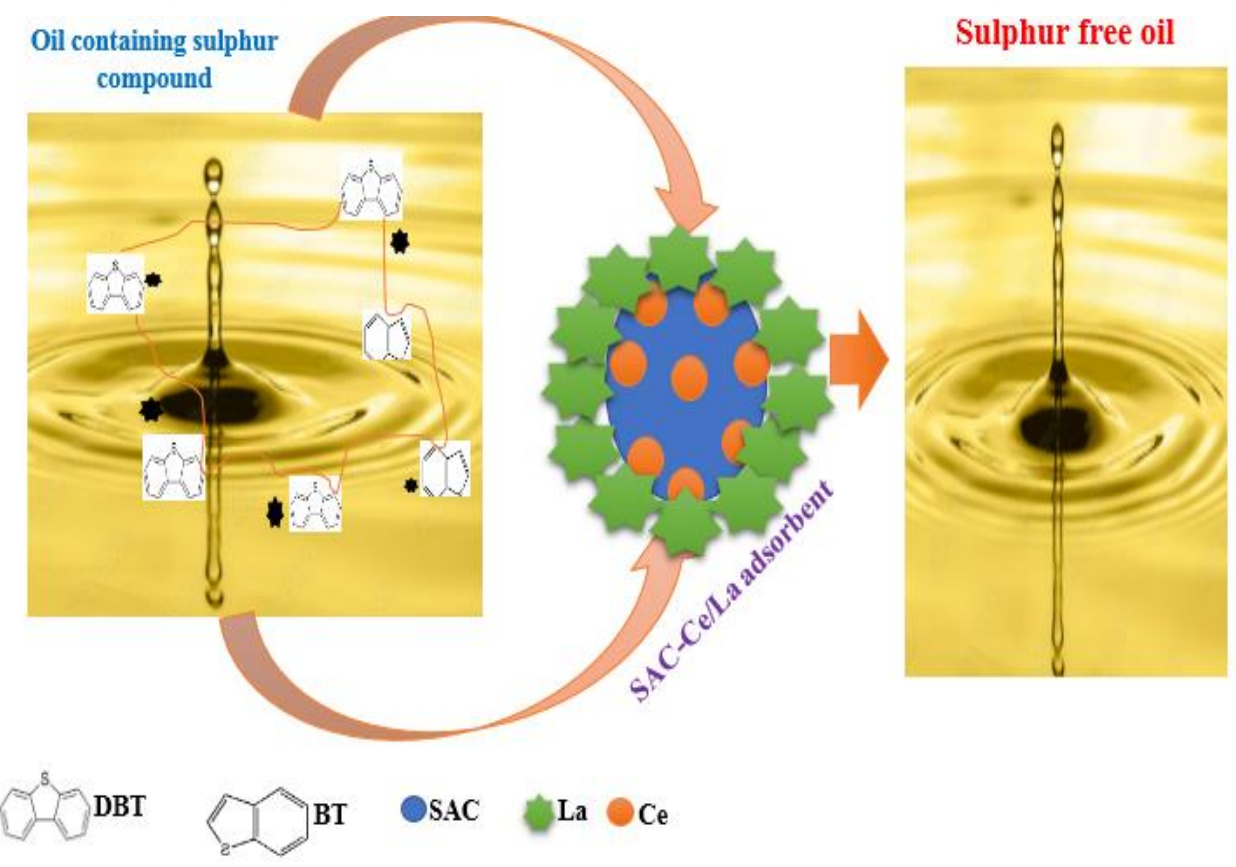


Figure 14: Mechanism of adsorption for DBT/BT over SAC-Ce/La adsorbent

ISSN (Online):0493-2137

E-Publication: Online Open Access Vol: 56 Issue: 06:2023

DOI: 10.5281/zenodo.17275786

4. CONCLUSION

The impact of NPs-support on the surface of AC adsorbents was investigated. SAC-Ce/La is a potential adsorbent for liquid fuels' desulphurization, based on the results of this study.

Evaluating the physicochemical parameters of the blank SAC-Ce/La with those of the BT/DBT loaded SAC-Ce/La, confirms the occurrence of BT/DBT on the surface of the adsorbent. Finally, the surface area, bimetallic nanocomposite, surface functional groups and pore volume of the SAC-Ce/La improved the adsorption capability of the ordinary SAC for DBT/BT removal.

Modifications in the adsorbents chemical composition, the acidic character of Ce nanooxide, and the crystalline behavior of La nano-oxide are all responsible for the enhanced adsorptive performance of the adsorbent. The Freundlich isotherm model and heterogeneous adsorption on the surface best described the equilibrium data.

Due to its high efficiency, simplicity, and eco-friendliness, SAC-Ce/La will find practical uses in the petroleum industry. Thermal regeneration of the SAC-Ce/La produced excellent results, thus indicating the potential of using the SAC-Ce/La at a large-scale. The breakthrough graphs show that the selectivity of the modified adsorbent for BT is < than that of DBT.

Author Contribution

Babalola Aisosa Oni: Conceived the idea, carried out the experimentation, Made the first draft copy of the manuscript. **Samuel Eshorame Sanni**: Made useful contributions at different stages of the research, Involved in recomposing key sections of the manuscript, and general editing of manuscript. **Olusegun Stanley Tomomewo**: Made very vital/useful observations at the experimental design and experimentation stages. Oyinkepreye David Orodu and Oboroghene T. Olomukoro: Data curation, Result analyses.

Funding: No funding was given to this research.

Data availability: All data generated and analyzed during our study are included in this article.

Declarations

Ethics approval: Not applicable.

Consent to participate: Not applicable.

Consent for publication: Not applicable.

Competing interests: The authors declare no competing interests.

Reference

- A.A. Olajire, J.J. Abidemi, A. Lateef, N.U. Benson, Adsorptive desulphurization of model oil by Ag nanoparticles-modified activated carbon prepared from brewer's spent grains, Journal of Environmental Chemical Engineering 5 (2017) 147–159.
- B.A Oni; S. E Sanni, S.O Dahunsi, B.C Egere, Decaffeination of wastewater using activated carbon produced from velvet tamarind-pericarp (*Dialium Guineense*), (2021): International Journal of Phytoremediation, DOI:10.1080/15226514.2021.1950118.

ISSN (Online):0493-2137

E-Publication: Online Open Access

Vol: 56 Issue: 06:2023

DOI: 10.5281/zenodo.17275786

- C. Marín-Rosas, L.F. Ramírez-Verduzco, F.R. Murrieta-Guevara, G. Hernández- Tapia, L.M. Rodríguez-Otal, Desulphurization of low sulphur diesel by adsorption using activated carbon: adsorption isotherms, Ind. Eng. Chem. Res. 49 (2010) 4372–4376.
- 4) Y. Guoxian, C. Hui, L. Shanxiang, Z. Zhongnan, Deep desulphurization of diesel by catalytic oxidation, Chem. Eng. China 1 (2) (2007) 162–166.
- 5) J. Wang, F. Xu, W. Xie, Z. Mei, Q. Zhang, J. Cai, W. Cai, The enhanced adsorption of dibenzothiophene onto cerium/nickel-exchanged zeolite Y, J. Hazard. Mater. 163 (2009) 538–543.
- 6) J.M. Palomino, D.T. Tran, J.L. Hauser, H. Dong, S.R.J. Oliver, Mesoporous silica nanoparticles for high-capacity adsorptive desulphurization, J. Mater. Chem. A 2 (2014) 14890–14895.
- P. Misra, S. Badoga, A. Chenna, A.K. Dalai, J. Adjaye, Denitrogenation and desulphurization of model diesel fuel using functionalized polymer: charge transfer complex formation and adsorption isotherm study, Chem. Eng. J. 325 (2017) 176–187.
- 8) Oni, B.A; Abatan, O.G, Busari, A., Olayemi Odunlami, O., Nweke, C., Production and characterization of activated carbon from pineapple waste for treatment of kitchen wastewater, *Desalination and Water Treatment*, 183 (2020) 413–424.
- 9) A.M. Moreira, H.L. Brandao, F.V. Hackbarth, D. Maass, A.A.U. de Souza, S.M.A.G.U. de Souza, Adsorptive desulphurization of heavy naphthenic oil: equilibrium and kinetic studies, Chem. Eng. Sci. 172 (2017) 23-31.
- 10) S.K. Thaligari, V.C. Srivastava, B. Prasad, Adsorptive desulphurization by zinc-impregnated activated carbon: characterization, kinetics, isotherms, and thermodynamic modeling, Clean Technol. Environ. Policy 18 (2016) 1021–1030.
- 11) F. Subhan, S. Aslam, Z. Yan, M. Ikram, S. Rehman, Enhanced desulphurization characteristics of Cu-KIT-6 for thiophene, Microporous Mesoporous Mater. 199 (2014) 108–116.
- 12) L. Xiong, X. Yan, P. Mei, Synthesis and Characterization of a ZrO₂ /AC Composite as a Novel Adsorbent for Dibenzothiophene. Adsorption Science and Technology (2010) 28(4):341-350.
- 13) Z. Yan, Wang, Z, Zou, J Liu, R., L; Zhang, Z; Wang, X (2012). Hydrothermal Synthesis of CeO nanoparticles on Activated Carbon with Enhanced Desulphurization Activity. Energy & Fuels, 26(9), 5879–5886. Doi: 10.1021/ef301085w.
- 14) S. Sumathi, S. Bhatia, KT, Lee, AR Mohamed. Selection of best impregnated palm shell activated carbon (PSAC) for simultaneous removal of SO₂ and NOx. Journal of Hazardous Materials. 176(1-3) (2010):1093–6.
- A. Mansouri, A.A. Khodadadi, Y. Mortazavi, Ultra-deep adsorptive desulphurization of a model diesel fuel on regenerable Ni–Cu/γ-Al₂O₃ at low temperatures in absence of hydrogen, J. Hazard. Mater. 271 (2014) 120–130.
- M.K. Nazal, M. Khaled, M.A. Atieh, I.H. Aljundi, G.A. Oweimreen, A.M. Abulkibash, the nature and kinetics of the adsorption of dibenzothiophene in model diesel fuel on carbonaceous materials loaded with aluminum oxide particles, Arabian J. Chem. (2015), doi: http://dx.doi.org/10.1016/j. arabjc.2015.12.003.
- 17) A.A. Adeyi, I.T. Popoola, A.S. Yusuff, A.S. Olateju, Kinetics analysis and dosage effect of manganese dioxide adsorbent on desulphurization of crude oil, J. Bioprocess. Chem. Eng. 2 (2014) 1–6.
- 18) C.S Song; X. Ma. New Design Approaches to Ultra-clean Diesel Fuels by Deep Desulphurization and Deep Dearomatization. Appl. Catal. B 2003, 41, 207-238.

ISSN (Online):0493-2137

E-Publication: Online Open Access

Vol: 56 Issue: 06:2023

DOI: 10.5281/zenodo.17275786

- 19) L. Yang, Y. Wang, D. Huang, G. Luo, Y. Dai Preparation of high-performance adsorbents by functionalizing mesostructured silica spheres for selective adsorption of organosulphur compounds Ind. Eng. Chem. Res., 46 (2007), 579-583
- 20) H.T. Kim, K.W. Jun, S.M. Kim, H.S. Potdar, Y.S. Yoon Co-precipitated Cu/ZnO/Al₂O₃ adsorbent for removal of odorants t-butylmercaptan (TBM) and tetrahydrothiophene (THT) from natural gas Energy Fuels, 20 (2006), 2170-2173.
- 21) M. Masuda, O. Okada, T. Tabata, Y. Hirai, H. Fujita. Method of desulphurization of hydrocarbons. US Patent 6,042,798; 2000.
- M. Shakirullah, I. Ahmad; M. Ishaq, W. Ahmad, (2009). Study on the Role of Metal Oxides in Desulphurization of Some Petroleum Fractions. Journal of the Chinese Chemical Society, 56(1), 107– 114. doi:10.1002/jccs.200900015
- 23) H. Chen, Y. Wang, F.H. Yang, R.T. Yang, Desulphurization of high-sulphur jet fuel by mesoporous π-complexation adsorbents, Chem. Eng. Sci. 64 (2009) 5240–5246.
- 24) H. Song, Y. Chang, X. Wan, M. Dai, H. Song, Z. Jin, Equilibrium, kinetic, and thermodynamic studies on adsorptive desulphurization onto CulCelVY zeolite, Ind. Eng. Chem. Res. 53 (2014) 5701–5708.
- 25) M. Ishaq, S. Sultan, I. Ahmad, H. Ullah, M. Yaseen, A. Amir, Adsorptive desulphurization of model oil using untreated, acid activated and magnetite nanoparticles loaded bentonite as adsorbent, J. Saudi Chem. Soc. (2015) 1–9.
- 26) L. Xiong, X Yan, P. Mei (2010). Synthesis and Characterization of a ZrO₂/AC Composite as a Novel Adsorbent for Dibenzothiophene. Adsorption Sci. & Tech, 28(4), 341–350. doi:10.1260/0263-6174.28.4.341
- 27) J.A. Arcibar-Orozco, J.R. Rangel-Mendez, T.J. Bandosz, Desulphurization of model diesel fuel on activated carbon modified with iron oxyhydroxide nanoparticles: effect of tert-butylbenzene and naphthalene concentrations, Energy Fuels 27 (2013) 5380–5387.
- 28) P. Tan, J.-X. Qin, X.-Q. Liu, X.-Q. Yin, L.-B. Sun, Fabrication of magnetically responsive core–shell adsorbents for thiophene capture: AgNO₃-functionalized Fe₃O₄@ mesoporous SiO₂ microspheres, J. Mater. Chem. A. 2 (2014) 4698–4705.
- 29) C. Yu, J.S. Qiu, Y.F. Sun, X.H. Li, G. Chen, Z. Bin, Adsorption removal of thiophene and dibenzothiophene from oils with activated carbon as adsorbent: effect of surface chemistry, J. Porous Mater. 15 (2008) 151–157.
- 30) X. Yang, L.E. Erickson, K.L. Hohn, P. Jeevanandam, K.L. Klabunde, Sol-gel Cu- Al₂O₃ adsorbents for selective adsorption of thiophene out of hydrocarbon, Ind. Eng. Chem. Res. 45 (2006) 6169–6174.
- 31) K. Tang, X. Hong, Y. Zhao, Y. Wang, Adsorption desulphurization on a nanocrystalline NaY zeolite synthesized using carbon nanotube template growth, Pet. Sci. Technol. 29 (2011) 779–787.
- 32) M. Mohammadian, M.R. Khosravi-Nikou, A. Shariati, M. Aghajani, Model fuel desulphurization and denitrogenation using copper and cerium modified mesoporous material (MSU-S) through adsorption process, Clean Technol. Environ. Policy. (2018) 1–18.
- 33) S. Yosuke, S. Kazuom, C. Ki-Hyouk, K. Yozo, M. Isao, two step adsorption process for deep desulphurization of diesel oil, Fuel 84 (7–8) (2005) 903–910.
- 34) X. Xu, S. Zhang, P. Li, Y. Shen, Desulphurization of Jet-A fuel in a fixed-bed reactor at room temperature and ambient pressure using a novel selective adsorbent, Fuel 117 (2014) 499–508.
- 35) J.-H. Shan, X.-Q. Liu, L.-B. Sun, R. Cui, Cu-Ce bimetal ion-exchanged Y zeolites for selective adsorption of thiophenic sulphur, Energy Fuel 22 (2008) 3955–3959.

ISSN (Online):0493-2137

E-Publication: Online Open Access

Vol: 56 Issue: 06:2023

DOI: 10.5281/zenodo.17275786

- 36) B.A. Oni, S.E Sanni Cationic graphene-based polymer composite modified with chromium-based metal-organic framework [GP/MIL-53(Cr)] for the degradation of 2,4-dichlorophenol in aqueous solution, Materials Today Sustainability 18 (2022) 100134.
- 37) I. Ahmed, S.H. Jhung, Adsorptive desulphurization and denitrogenation using metalorganic frameworks, J. Hazard. Mater. 301 (2016) 259–276.
- 38) G. Bakhtiari, M. Abdouss, M. Bazmi, S. Royaee, Optimization of sulphur adsorption over Ag-zeolite nanoadsorbent by experimental design method, Int. J. Environ. Sci. Technol. 13 (2016) 803–812.
- 39) X. Sun, B.J. Tatarchuk, Photo-assisted adsorptive desulphurization of hydrocarbon fuels over TiO₂ and Ag/TiO₂, Fuel 183 (2016) 550–556.
- 40) A.S. Tawfik, I.D. Gaddafi, S. Taye Damola, Nanocomposites and hybrid materials for adsorptive desulphurization, in: A.S. Tawfik (Ed.), Applying Nanotechnology to the Desulphurization Process in Petroleum Engineering, IGI Global, Hershey, PA, USA 2016, pp. 129–153.
- 41) M. Yu, N. Zhang, L. Fan, C. Zhang, X. He, M. Zheng, Z. Li, Removal of organic sulphur compounds from diesel by adsorption on carbon materials, Rev. Chem. Eng. 31 (2015) 27–43.